Zhu *et al. Reproductive Biology and Endocrinology* (2025) 23:62
https://doi.org/10.1186/s12958-025-01395-y

Reproductive Biology and Endocrinology

RESEARCH Open Access

Comparative analysis of endometrial gland imaging and pinopode detection for assessing endometrial receptivity

Min-bo Zhu[1], Bei-lei Chen[1], Meng Cen[1], Li-ping Chen[1] and Zheng Shi[1*]

Abstract

Background This study aimed to obtain high-resolution endometrial gland images under high-definition hysteroscopy from in vitro fertilization and embryo transfer (IVF-ET) patients and perform image recognition to analyze their density and opening size. Concurrently, the number and morphology of pinopodes in the endometrial samples were observed using scanning electron microscopy (SEM). The objective was to compare the correlation between the two methods in evaluating endometrial receptivity and predicting pregnancy outcomes and to assess the consistency between the quantitative curves and pregnancy outcomes of the two methods in the cohort study.

Methods 67 patients undergoing hysteroscopic surgery who had undergone controlled ovarian hyperstimulation treatment within 1–3 menstrual cycles before the surgery were selected. Hysteroscopic exploration was performed on the 3–5 days after ovulation (during the implantation window period). Endometrial images and tissues were collected under hysteroscopy. The endometrial glands were counted, the sizes of gland openings were calculated using an image recognition algorithm, and the number and morphology of endometrial pinopodes were observed through SEM. All patients underwent embryo transfer surgery within 1–3 menstrual cycles after hysteroscopy. Patients were divided into pregnancy and non-pregnancy groups based on pregnancy outcomes. The density and size of endometrial glands, as well as the number and morphology of pinopodes were compared between the two groups.

Results The endometrial gland density and the size of the endometrial gland opening in the pregnancy group were higher than that in the non-pregnancy group ($P < 0.05$). In contrast, both the average pinopode count per image and the developmental maturity grading of pinopodes were significantly higher in the pregnancy group compared to the non-pregnancy group.

Conclusions Both hysteroscopic endometrial gland image recognition technology and pinopode detection can effectively reflect endometrial receptivity and predict pregnancy outcomes. However, image recognition technology has clear economic and promotional advantages.

Clinical trial number Not applicable.

Keywords Endometrial gland, Image recognition, Pinopodes, In vitro fertilization and embryo transfer, Endometrial receptivity

*Correspondence:
Zheng Shi
qiaowei0904@163.com

[1]Ningbo Municipal Key Laboratory of Clinical Gynecology, Department of Gynecology, Women and Children's Hospital of Ningbo University, Ningbo, Zhejiang 315012, China

Background

In vitro fertilization and embryo transfer (IVF-ET) has emerged as an essential treatment for infertility. The success of IVF-ET treatment is primarily determined by the quality of embryos and endometrial receptivity. Endometrial receptivity refers to the endometrium's ability to support embryo implantation, which is a dynamic and regulated process. Recent advances in reproductive medicine have identified pinopodes as highly sensitive markers of endometrial receptivity. Pinopodes are specialized structures formed by the fusion of microvilli on the surface of endometrial epithelial cells. Their abundance and maturity are indicative of a favorable endometrial environment, which is essential for the localization, attachment, and implantation of the blastocyst [1].

Pinopodes develop through three stages: development, maturity, and degeneration. They appear in the mid-secretory phase (6–9 days after ovulation) and last for less than 48 h, corresponding with the endometrial "implantation window" [2]. The presence and maturity of pinopodes are closely associated with the optimal expression of adhesion molecules, cytokines, and growth factors, all of which are critical for embryo invasion and successful implantation. Furthermore, pinocytosis, the process by which endometrial cells internalize various molecules such as nutrients, cytokines, and growth factors, plays an integral role in creating a favorable environment for embryo invasion during the implantation window [3]. This dynamic process is essential for regulating the endometrial stroma and facilitating the transport of molecules crucial for embryo attachment and invasion.

Traditionally, endometrial receptivity has been evaluated through methods like ultrasound, biopsy, and endometrial proteomics [4]. However, these methods have limitations, such as invasiveness and lack of real-time results. In contrast, the use of high-definition hysteroscopy combined with image recognition technology offers a non-invasive, real-time, and cost-effective method for assessing endometrial gland density and gland opening size. In this study, we employed a high-definition hysteroscopy to capture endometrial gland images and applied an image recognition algorithm to analyze gland density and opening size [5].

This study aimed to assess endometrial receptivity by integrating two complementary methodologies and comparing the effectiveness of image recognition technology and pinopode detection in predicting implantation success. Concurrently, pinopode morphology was assessed through scanning electron microscopy (SEM) to further evaluate the correlation between endometrial gland features and pinopode development. Pregnancy outcomes were subsequently monitored to evaluate the predictive value of these two methodologies in determining endometrial receptivity.

Materials and methods

Patient selection

This study included 67 infertility patients aged 23–34 years receiving IVF-ET treatment at the Reproductive Medicine Center of Ningbo Women and Children's Hospital from January 2020 to December 2020. Of the patients, 30 experienced primary infertility and 37 were diagnosed with secondary infertility lasting 1–8 years. The menstrual cycle of each patient was regular. Exclusion criteria for this study involved patients with abnormal uterine outcomes, including endometrial polyp, myoma, endometriosis, adenomyosis, intrauterine adhesion, and endocrine-related disease, or those who had undergone uterine and ovarian surgery. Additionally, all patients underwent controlled ovarian hyperstimulation therapy during the 1–3 menstrual cycles preceding the hysteroscopic procedure, and embryo transfer was deferred until after the surgery. Ovulation monitoring was conducted during the month of hysteroscopic surgery, and a hysteroscopic examination was carried out 3–5 days post-ovulation. During the surgery, no abnormal findings such as endometrial polyps or intrauterine adhesions were found, and within 3 menstrual cycles following hysteroscopic surgery, embryo transfer was conducted. In the pregnancy group, 45 patients were identified as having clinical intrauterine pregnancy via ultrasound. The diagnostic criteria for early pregnancy involved an intrauterine pregnancy, with an enlarged gestational sac (mean gestational sac diameter > 10 mm), based on a B-type ultrasound examination. Missed abortion, early induced abortion, premature delivery, full-term delivery, and mid-term induced labor were all considered pregnancy outcomes. The non-pregnancy group consisted of 22 patients, including those with extrauterine pregnancies, such as those with human chorionic gonadotropin (hCG)-negative pregnancies, chemical pregnancy (hCG-positive with no pregnancy seen on ultrasound, followed by natural menstruation), as well as ectopic pregnancy (extrauterine pregnancy; excluding cornual pregnancy).

Hysteroscopic procedure

The procedure was scheduled 3–5 days following ovulation, verified through ovulation monitoring (± 2 days from the window of implantation). Starting on the 10th day of the menstrual cycle, ultrasound monitoring was performed at 2–3 day intervals. When the average follicle diameter reached 20 mm, 5000 U of HCG was injected. Two days later, a repeat ultrasound was conducted to assess whether ovulation had occurred. Once ovulation was confirmed, hysteroscopic surgery was scheduled within 3–5 days at Ningbo Women and Children's Hospital by the Gynecologists using intravenous anesthesia with propofol as well as laryngeal mask-assisted

ventilation. The presence of any deformities, adhesions, or space-occupying lesions in the cervical canal and uterine cavity was visualized and determined by positioning a hysteroscope.

A High-definition hysteroscopic imaging was performed using a rigid hysteroscope (KARL STORZ SE & Co. KG, Germany) equipped with a small-diameter outer sheath of approximately 5 mm and a high-definition optical system delivering images at 1920 × 1080 resolution. This setup allowed for precise, real-time image acquisition of the endometrium. The general anesthesia was used to ensure patient comfort, minimize movement during the procedure, and allow for precise and reproducible positioning of the hysteroscope within the uterine cavity.

During the procedure, the uterine fundus was used as the focal point for image acquisition, and an epidural catheter with scale marks was employed to accurately measure the distance between the fundus and the hysteroscopic lens. This approach allowed for precise alignment of the hysteroscope for imaging and accurate endometrial tissue sampling. After capturing the required images, micro-grasping forceps were placed through the hysteroscopic operating channel to grab endometrial tissue at the image collection site for further analysis.

All surgeons involved in the procedure were trained in the standard operating protocols to ensure that the procedure was conducted safely, precisely, and in accordance with the required standards.

Frozen embryo transfer and endometrial Preparation

For patients with regular menstrual cycles, follicular and endometrial development was monitored starting from day 10 of menstruation. Once a dominant follicle was observed, continuous monitoring was conducted, and urinary LH or corresponding hormone levels were used to assess follicular maturity; if necessary, HCG was administered to induce ovulation. After ovulation, the embryo transfer timing was determined based on the frozen embryo's culture duration, and during the transfer window, ultrasound confirmed that the endometrium had reached a thickness of ≥ 8 mm, which was considered acceptable for transfer. For patients in natural cycles who did not ovulate or in artificial cycles with suboptimal endometrial preparation, HMG was started on days 3–5 of the menstrual cycle; when the follicle developed to approximately 1.8–2.0 cm, HCG was injected, and then, based on the ovulation time and the embryo's culture duration, the transfer time was determined, ensuring that the endometrium was ≥ 8 mm on ultrasound during the transfer window.

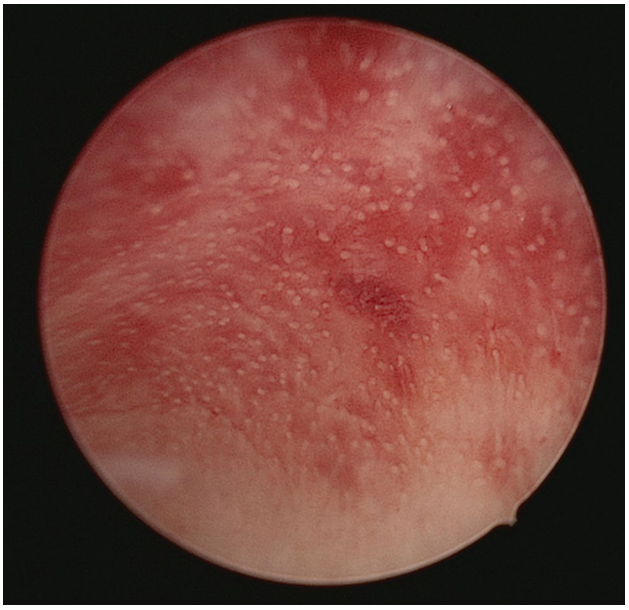

Fig. 1 The origin endometrial image (1080 × 1080 pixels)

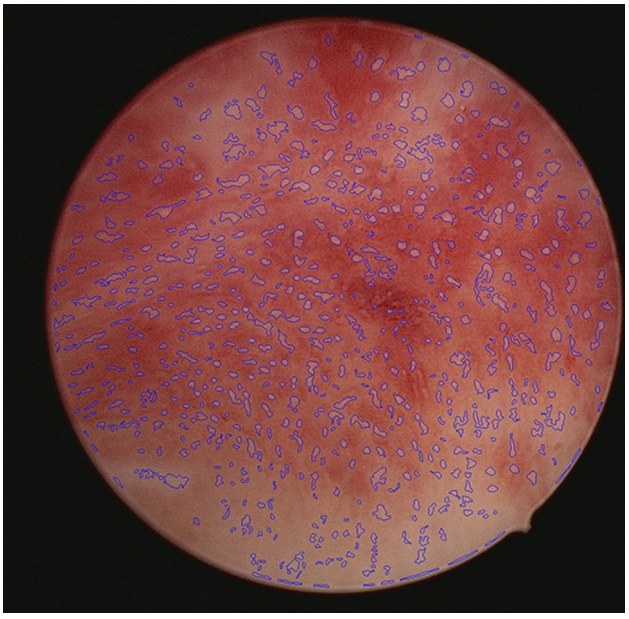

Fig. 2 The image processed using the algorithm. The glands were marked and counted. Pixel points of the glands were measured to calculate the opening size of endometrial glands

Endometrial gland image recognition

The endometrial images were cut into squares with a resolution of 1080 × 1080 pixels (Fig. 1), and for recognizing, marking, and counting the endometrial glands, an endometrial gland opening labeling algorithm was adopted to process the images (Fig. 2). The calculation method for the opening size of endometrial glands was to recognize all glands in the image, calculate the total pixel points

(pp) occupied by all glands, and then calculate the average value.

Endometrial pinopode detection

Endometrial tissues obtained during surgery were rinsed three times with physiological saline, and a 2.5% glutaraldehyde fixing solution (pH 7.2–7.4) at least 10 times than the volume of the tissues was added. The tissues were stored at a temperature of 4℃ and made into electron microscope samples. After that, scanning electron microscopy with a magnification of 3000 times (HITACHI SU8010) was used to observe the number, morphology, and coverage rate of the pinopodes at a magnification of 3000 times. The morphology of the pinopodes was divided into four levels based on the grading of their developmental status: pre-development (Fig. 3), developing (Fig. 4), fully developed (Fig. 5), and degenerating (Fig. 6). The coverage rate of the pinopodes was the percentage of the area of the pinopodes process to the area of the endometrium. Each sample was randomly selected from 8 areas, and the pinopodes were counted. The average number of pinopdes was calculated for each sample, and the scoring and grading were based on the coverage rate of pinopodes. Zero was scored for completely uncovered (0%), one was scored for slightly covered (≤ 20%), two was scored for moderately covered (21–50%), and three was scored for extensively covered (> 50%), Finally, based on the pregnancy outcome, a χ^{2-} test was performed on the grading of the pinopodes.

Statistical methods

Data analysis was performed using IBM SPSS Statistics version 19.0 (IBM Corporation, Armonk, NY, USA). Continuous variables were expressed as mean ± standard deviation (SD) and compared between groups using the independent-samples t-test. Categorical variables were analyzed using the chi-square test. In addition, Pearson's bivariate correlation analysis was employed to evaluate the relationships among the variables. A two-tailed p-value of less than 0.05 was considered statistically significant.

Results

Comparison of general information between two groups

The mean ages, endometrial thickness on the day of embryo transfer, body mass index (BMI), length of infertility years, and number of embryo transferred did not exhibit any statistical significance between the non-pregnancy and pregnancy groups (all $P > 0.05$, Table 1). The pregnancy group involved 18 cases of primary and 27 of secondary infertility, while in the non-pregnancy group, 11 cases were diagnosed with primary infertility and secondary infertility, respectively. The two groups presented

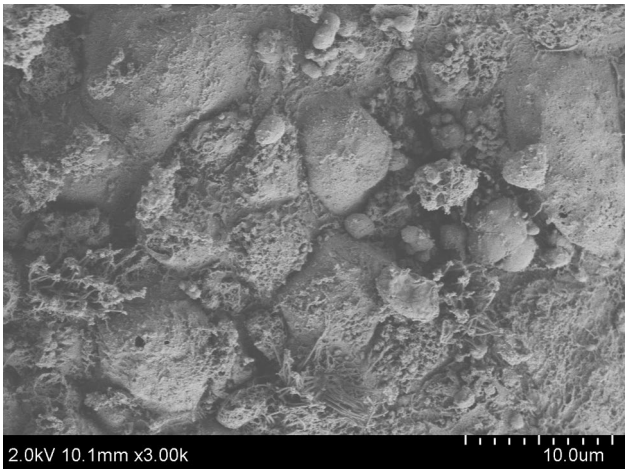

Fig. 3 Before the development of the pinopodes, their volumes are small, and surface microvilli are visible

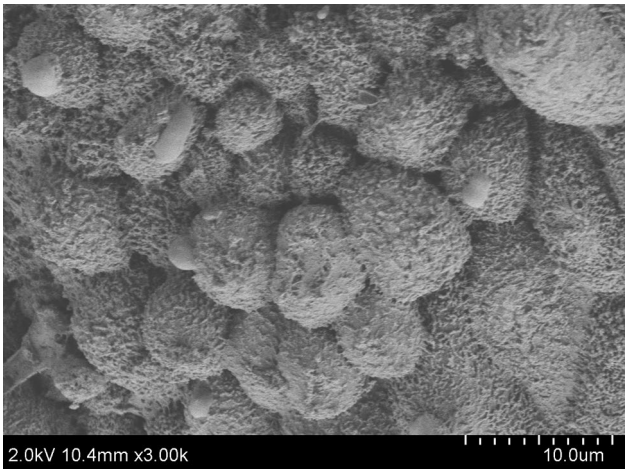

Fig. 4 During the development of pinopodes, the volumes gradually fill up, and the villi shorten

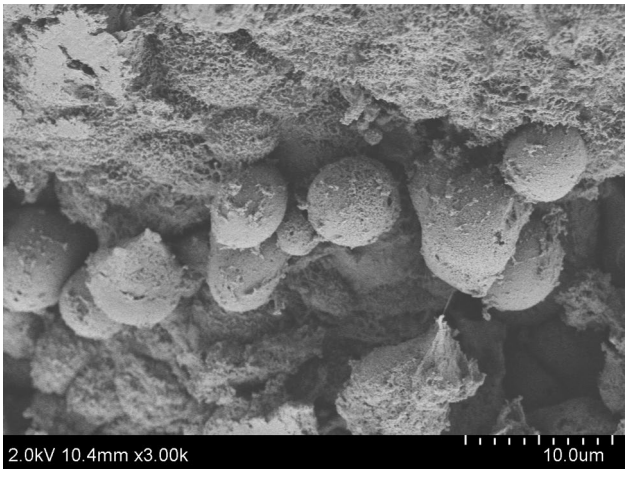

Fig. 5 The pinopoodes are fully developed, with a smooth surface and almost disappeared villi

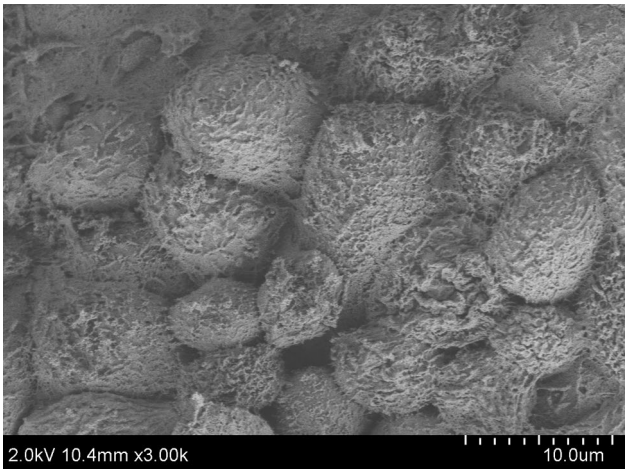

Fig. 6 Degenerating pinopodes, with wrinkles and microvilli reappearing on the surface, increasing in volume

no statistical significance in primary and secondary infertility ($\chi^2 = 0.602$, $P = 0.438$, Table 2).

Comparison of endometrial gland count between two groups

All endometrial images were processed using the image recognition algorithm, and the number of endometrial glands was identified and counted. Simultaneously, the total number of pixels occupied by all endometrial glandular openings was calculated to determine the mean size, expressed in pixels. The calculation formula is ($\text{gland opening size} = \frac{\text{pixels occupied by all glandular openings}}{\text{total number of glandular openings}}$). The pregnancy group exhibited a higher number of endometrial glands and size of endometrial gland openings as opposed to the non-pregnancy group ($P < 0.05$, Table 3).

Comparison of the count numbers and developmental status grading of pinopodes between two groups

In contrast to the non-pregnancy group, a higher average count of pinopodes was observed in the pregnancy group ($P < 0.05$, Table 3). The developmental status grading was considerably different between the non-pregnancy and pregnancy groups ($\chi^2 = 1.196$, $P = 0.011$, Table 4).

Table 2 Comparison of primary infertility and secondary infertility between groups

	Primary infertility	Secondary infertility	Compare Results
Pregnancy group	18	27	$\chi^2 = 0.602$
Non-pregnancy group	11	11	$P = 0.438$ (bilateral)

Table 3 Comparison of endometrial gland count, gland opening size and pinopodes count between two groups($\bar{x} \pm s$)

	Endometrial gland count (*n*)	Gland opening size (PP)	Count of pinopodes (*n*/pic, ESM at 3000X magnification)
Pregnancy group	130.27 ± 29.46	220.44 ± 81.32	18.04 ± 3.46
Non-pregnancy group	88.05 ± 25.63	152.36 ± 74.0	11.82 ± 2.47
P	< 0.001	< 0.001	< 0.001

Table 4 Comparison of the developmental status grading of pinocytosis between two groups of patients

	Completely uncovered (0 points)	slightly coverage (1 point)	Moderate coverage (2 points)	Extensive coverage (3 points)	Compare Results
Pregnancy group	0	17	17	11	$\chi^2 = 1.196$,
Non-pregnancy group	5	6	6	5	$P = 0.011$ (bilateral)

Comparison of the correlation between endometrial glandular count, glandular opening size, and pinopode count

There was a statistically significant positive correlation of endometrial glandular count, and glandular opening size with pinocytosis count ($P < 0.05$, Table 5).

Discussion

Throughout the multiple stages of IVF-ET treatment, continuous advancements in ovulation induction therapy and the progressive refinement of artificial insemination technology have led to an egg fertilization rate exceeding 70%, along with a gradual increase in the rate

Table 1 Comparison of age, length of infertility, BMI, endometrial thickness on embryo transfer day, and number of embryos transferred between the two groups ($\bar{x} \pm s$)

	Age (years)	Length of infertility (years)	Body mass index (kg/m^2)	Endometrial thickness on the day of embryo transfer (mm)	Number of embryo transfered
Pregnancy Group	28.16 ± 3.34	2.95 ± 1.10	21.75 ± 3.74	11.28 ± 1.33	1.38 ± 0.49
non-pregnancy Group	27.73 ± 3.60	2.94 ± 0.96	22.31 ± 3.08	11.35 ± 1.56	1.45 ± 0.51
P	0.640	0.990	0.550	0.880	0.550

Table 5 Comparison of correlation between endometrial glandular count, glandular opening size, and pinopodes count

		Endometrial gland count (*n*)	Gland opening size (PP/pic)
Count of pinopodes (n/pic, ESM at 3000X magnification)	Pearson correlation coefficient	0.468	0.456
	P	< 0.001	< 0.001

of high-quality embryos. Simultaneously, with the ongoing maturation of sequential blastocyst culture technology, it is now possible to extend and cultivate embryos in vitro to the blastocyst stage [6]. However, the pregnancy rate after embryo transfer has not significantly improved, with the cumulative clinical pregnancy rate remaining around 55–65%. The discrepancy between the embryo acquisition rate and the pregnancy rate underscores the critical role of endometrial receptivity and ovarian responsiveness after embryo transfer in determining pregnancy outcomes, with endometrial receptivity being the most crucial factor [7]. Currently, ultrasound examination remains the most commonly used method for evaluating endometrial receptivity in clinical practice [8]. In addition, various methods, such as endometrial proteomics and endometrial lipid mediators are available but each has certain limitations [9, 10].

As a widely recognized marker for endometrial receptivity testing, the pinocytosis process has been confirmed in this study. In this study, patients in the pregnancy group had significantly higher scores for pinocytosis count and developmental status grading than those in the non-pregnancy group, indicating that if embryo transfer time is determined based on the results of pinocytosis testing, a higher clinical pregnancy rate can be achieved. However, due to the low popularity of high-resolution scanning electron microscopy equipment, expensive detection costs, and poor timeliness, the detection of pinopodes, although a suitable method for evaluating endometrial receptivity, cannot be widely applied.

In comparison to previous studies, such as Sakumoto et ^{al} [11]., which examined the mid-secretion endometrial morphology through hysteroscopy, our study incorporates a more quantitative approach. While previous study relied on subjective evaluation of endometrial morphology using visual assessment of blood vessel distribution and glandular opening size, our study integrates image recognition technology with hysteroscopy, offering a non-invasive, real-time, and objective alternative. Furthermore, while pinopodes were assessed using SEM in previous studies, our image recognition technology allows for quantification of endometrial gland density and opening size, providing a cost-effective and clinically feasible method for assessing endometrial receptivity. Unlike traditional techniques, which can be time-consuming and subjective, our methodology offers a more practical solution for routine clinical use.

At present, high-definition hysteroscopic surgical equipment is widely used, and the resolution of endometrial images has reached the level of 10 micrometers. Combining with the increasingly developed computer software and hardware technology, it is possible to perform computer software recognition on endometrial images. In 2018, our research team used a published image recognition algorithm to verify the feasibility of using image recognition technology to obtain endometrial gland density to evaluate endometrial receptivity [12].

On the basis of the previous study, this study added the recognition of the size of endometrial glandular openings. It used SEM to detect and grade pinopodes in endometrial tissue obtained during hysteroscopy, verifying the effectiveness of pinopode detection in endometrial receptivity. In this study, we analyzed the correlation of the size of the endometrial gland opening and the endometrial gland count with the results of pinocytosis detection. The result indicated a significant correlation between the three. Therefore, using image recognition technology to evaluate endometrial receptivity has high feasibility while also has real-time and economical features compared to pinopode detection making it a valuable method for widespread clinical application.

Our study not only demonstrates a significant correlation between endometrial gland imaging parameters and traditional pinopode detection but also highlights several key strengths. A major strength of this study is the innovative integration of high-definition hysteroscopy with an automated image recognition algorithm. This novel approach enables objective, real-time quantification of endometrial gland density and glandular opening size—parameters that correlate strongly with established markers of endometrial receptivity as assessed by SEM-based pinopode evaluation. Unlike conventional methods that often rely on subjective interpretation and expensive, time-consuming SEM analysis, our method offers a cost-effective, reproducible, and accessible alternative for clinical practice. Moreover, the rigorous design involving a well-defined patient cohort and comprehensive statistical analysis further reinforces the reliability and clinical applicability of our findings. Overall, these strengths suggest that our image recognition technology could play a valuable role in optimizing embryo transfer timing and improving IVF-ET outcomes.

Although this study demonstrates the feasibility of image recognition technology for assessing endometrial receptivity, further research is needed to enhance its clinical utility. Future studies should validate this method in larger, multicenter trials to assess its generalizability. The integration of deep learning algorithms could improve

the accuracy, automation, and predictive value of this approach. Additionally, the development of laser measurement technologies for more precise image acquisition may enhance its accuracy. Ultimately, prospective clinical trials comparing the cost-effectiveness and clinical impact of this technology to traditional methods (e.g., ultrasound and biopsy) will be essential for its adoption in clinical practice.

Conclusion

In summary, the integration of high-definition hysteroscopy with image recognition technology provided a promising, non-invasive alternative for evaluating endometrial receptivity, with significant potential for clinical application in IVF-ET. This approach could aid in developing long-term embryo transfer plans, reduce medical expenses and embryo waste, and improve IVF-ET pregnancy rates.

Abbreviations

IVF-ET	In vitro fertilization and embryo transfer
SEM	Scanning electron microscopy
hCG	Human chorionic gonadotropin
pp	Pixel points

Acknowledgements

None.

Author contributions

MZ was responsible for data curation, formal analysis, obtaining funding, conducting investigations, planning the methodology, administering the project, and writing the original draft of the manuscript; LC also performed data curation and formal analysis, conducted investigations, designed the methodology, assisted the project, and was involved in reviewing and editing the manuscript; BC and MC were engaged in conducting formal analyses and investigations, obtaining resources, and performing validation; ZS and LC similarly conducted formal analyses and investigations, received resources, and performed validation; All authors collectively contributed to the conception and design of the study, and each read and approved the final manuscript.

Funding

This study is supported by Zhejiang Medical and Health Science and Technology Project (2024KY346); Ningbo Top Medical and Health Research Program (No.2024021020); Ningbo Clinical Medical Research Center for Gynecological Diseases (Grant numbers: 2024L002).

Data availability

The dataset supporting the conclusions of this article is available upon request. Please contact Dr. Zhu Minbo (zhuminbo@163.com).

Declarations

Consent of publication

Not applicable.

Institutional review board statement

The study was conducted in accordance with the Declaration of Helsinki and approved by the Ethics Committee of Ningbo Women and Children's Hospital (No. 20183282), and the requirement for written informed consent was waived owing to its retrospective design.

Competing interests

The authors declare no competing interests.

Received: 1 November 2024 / Accepted: 10 April 2025
Published online: 28 April 2025

References

1. D'Ippolito S et al. Expression of pinopodes in the endometrium from recurrent pregnancy loss women. Role of thrombomodulin and Ezrin. J Clin Med, 2020. 9(8).
2. Zhioua A, et al. [Morphometric analysis of the human endometrium during the implantation window. Light and transmission electron microscopy study]. J Gynecol Obstet Biol Reprod (Paris). 2012;41(3):235–42.
3. Srivastava A, et al. Profiles of cytokines secreted by isolated human endometrial cells under the influence of chorionic gonadotropin during the window of embryo implantation. Reprod Biol Endocrinol. 2013;11:116.
4. Miravet-Valenciano J, Ruiz-Alonso M, Simón C. *Modern Evaluation of Endometrial Receptivity*, in *Ultrasound Imaging in Reproductive Medicine: Advances in Infertility Work-up, Treatment and ART*, L.A. Stadtmauer and I. Tur-Kaspa, Editors. 2019, Springer International Publishing: Cham. pp. 357–366.
5. Yang S, Huang X, Min L, et al. Endometrial gland opening labelling algorithm under hysteroscopy based on morphological reconstruction. Beijing Biomedical Eng. 2015;10(5):468–71.
6. Glujovsky D, Farquhar C. Cleavage-stage or blastocyst transfer: what are the benefits and harms? Fertil Steril. 2016;106(2):244–50.
7. Demura TA, et al. [The role of inherited thrombophilia and undifferentiated connective tissue dysplasia syndrome in the pathogenesis of female infertility: A clinical and morphological study]. Arkh Patol. 2015;77(4):3–10.
8. Mayer RB, et al. The role of endometrial volume and endometrial and subendometrial vascularization parameters in a frozen embryo transfer cycle. Reprod Sci. 2019;26(7):1013–8.
9. Braga D, et al. Lipidomic profile as a noninvasive tool to predict endometrial receptivity. Mol Reprod Dev. 2019;86(2):145–55.
10. Hernandez-Vargas P, Munoz M, Dominguez F. Identifying biomarkers for predicting successful embryo implantation: applying single to multi-OMICs to improve reproductive outcomes. Hum Reprod Update. 2020;26(2):264–301.
11. Jain M, et al. Mucosal biomarkers for endometrial receptivity: A promising yet underexplored aspect of reproductive medicine. Syst Biol Reprod Med. 2022;68(1):13–24.
12. Zheng S, Minbo Z, Chunya T. Endometrial receptivity evaluation using hysteroscopic endometrial gland image recognition. Hum Fertil (Camb). 2023;26(5):1347–53.

Publisher's note